

Effect of thermomechanical treatment on the microstructure and mechanical properties of a nickel base superalloy heavily alloyed with substitution elements

V. M. Imayev^{†,1}, Sh. Kh. Mukhtarov¹, A. V. Logunov², A. A. Ganeev¹, R. V. Shakhov¹,

L. R. Shaikhutdinova³, R. M. Imayev¹

[†]vimayev@mail.ru

¹Institute for Metals Superplasticity Problems RAS, 39 S. Khalturin St., Ufa, 450001, Russia

²PJSC “UEC-Saturn”, 163 Lenina Av., Rybinsk, 152903, Russia

³Ufa State Aviation Technical University, 12 K. Marx St., Ufa, 450008, Russia

The work has been devoted to a study of the microstructure and mechanical properties of a novel heavily alloyed nickel base superalloy in cast and heat-treated (HT) and thermomechanically treated (TMT) conditions. The cast condition subjected to HT, including homogenization annealing, solid solution treatment and ageing, was characterized by a coarse γ grain size and uniformly distributed γ' precipitates with a size $d_{\gamma'} = 0.1 - 0.25 \mu\text{m}$. TMT included unidirectional two-step forging in a thick-walled can made of stainless steel, which provided high quasi-hydrostatic pressure during forging, and intermediate recrystallization annealing at subsolvus temperatures. The TMT condition was aged. TMT led to the uniform development of recrystallization processes and the formation of predominantly recrystallized microstructure with a γ grain size $d_{\gamma} = 2 - 50 \mu\text{m}$. Non-recrystallized areas with up to $100 \mu\text{m}$ in size were also observed. After TMT and ageing, the microstructure contained mostly dispersed γ' precipitates with a size of $d_{\gamma'} = 0.1 - 0.3 \mu\text{m}$. Tensile tests revealed that the strength properties in the TMT condition were by 20–70% higher than in the cast and HT condition. The TMT condition also showed an appreciably higher ductility than the HT condition. The following tensile properties were obtained at room temperature: $\sigma_{\text{UTS}}/\sigma_{0.2} = 1533/1083 \text{ MPa}$, $\delta = 11\%$ after TMT and ageing, and $\sigma_{\text{UTS}}/\sigma_{0.2} = 1015 - 1030/900 \text{ MPa}$, $\delta = 4.5 - 5.2\%$ after HT. Higher tensile properties after TMT are explained by the γ grain refinement, the high γ' phase content, and the solid solution strengthening due to heavy alloying with substitution elements. At the same time, the presence of topologically close-packed phases probably reduced the mechanical properties.

Keywords: nickel base superalloy, thermomechanical treatment, microstructure, mechanical properties.

1. Introduction

Heat-resistant nickel base superalloys are widely used as structural materials in gas turbine engines (GTE), in particular for manufacturing of turbine parts [1–4]. To increase the fuel efficiency of GTE, one tries to increase operating temperatures and loadings. That encourages the development of heavily alloyed nickel base superalloys with increased strength and heat resistance. With respect to polycrystalline nickel base superalloys, it is of interest to increase alloying with the elements forming the γ' phase and the substitution elements including refractory ones to provide solid-solution hardening [1–6]. However, heavily alloyed nickel base superalloys in the cast condition (after heat treatment) usually have rather low mechanical properties. The use of conventional hot working techniques is the challenging problem due to low hot workability of the superalloys. A heterogeneous structure and a strong dendritic segregation in the as-cast ingot limit the hot workability even at temperatures near the solvus temperature of the γ' phase. At the same time, achieving properly balanced mechanical

properties in heavily alloyed nickel base superalloys is not feasible without transformation of the as-cast ingot into the wrought billet leading to breaking up of the coarse grained as-cast structure and its transformation into a recrystallized structure.

To increase the hot workability of heavily alloyed nickel base superalloys produced by casting, preliminary homogenization and heterogenization heat treatment is usually applied to dissolve dendritic segregation and to enlarge the γ' precipitates in the course of their coagulation and spheroidization [1, 3, 4]. After that, the appropriate hot working scheme and temperature-strain rate conditions are selected. The relatively low stacking fault energy and the high content of γ' phase particles promote the dislocation accumulation during hot deformation and, therefore, a moderate strain value ($\epsilon \geq 1.2$) is typically required to achieve a recrystallized structure in nickel base superalloys during hot working. To provide the uniform development of recrystallization processes and the formation of a fine-grained structure, it is important to accurately select the temperature-strain rate conditions and the hot working scheme providing

all-round compression, such as hydroextrusion, compression in a thick-walled can, etc.

In the present work, the heavily alloyed nickel base superalloy SLZhS-1R was taken as a starting material. The superalloy was developed at PJSC “UEC-Saturn” (Rybinsk, Russia) using computer design and intended for use as the die material and the disk material for GTE with operating temperatures up to 800°C. The superalloy contains a higher amount (>35 wt.%) of substitution elements (Cr, Co, W) to provide effective solid solution hardening. The heat treatment prior to hot working and the temperature-strain rate conditions of the hot working were early determined elsewhere [7, 8].

The work was aimed at a comparative study of the microstructure and mechanical properties of the superalloy SLZhS-1R in the cast and heat treated (HT) and the cast and thermomechanically treated (TMT) conditions. To ensure high quasi-hydrostatic pressure during hot working, the TMT workpiece was encapsulated in a can made of a stainless steel.

2. Material and experimental methods

The nominal composition of the superalloy SLZhS-1R was Ni-47(Al, Cr, Co, Ta, W, Hf)-0.2(C, B) (wt.%). As-cast ingots with a size of $\varnothing 45 \times 270$ mm were manufactured and supplied by STC “Technologies of special metallurgy” Ltd, MISiS (Russia). The actual compositions of the ingots corresponded to the nominal composition of the superalloy.

The solvus temperature (T_s) of the γ' phase was determined via quenching experiments from temperatures near the γ' solvus temperature. It was defined as $T_s = 1185 \pm 5^\circ\text{C}$. The as-cast condition was subjected to HT consisting of homogenization annealing in the temperature range of 1100–1200°C followed by solid solution heat treatment with air cooling and ageing. Two-stage ageing was carried out at 1000 and 880°C followed by air cooling. The HT workpieces were used to prepare samples for tensile testing.

Other cast workpieces were subjected to homogenization and heterogenization annealing in the temperature range of 1100–1200°C followed by slow furnace cooling. After that, the heat-treated workpieces were encapsulated in thick-walled stainless steel cans and subjected to TMT, which included unidirectional forging in two stages under quasi-isothermal conditions with intermediate recrystallization annealing at a temperature slightly lower than the forging temperature. The workpiece preheating temperature was 1150°C, the die temperature was 930°C. The forging procedure was carried out with the strain rate of $\dot{\epsilon} \approx 10^{-2} \text{ s}^{-1}$, the total strain value during forging was $\epsilon \approx 1.4$. The forged workpieces were cooled in air and aged at 860 and 750°C followed by air cooling. The TMT workpieces were used to prepare samples for tensile testing.

Mechanical tensile tests were performed at temperatures of 20, 650 and 750°C. To do it, flat samples with the gauge section of $10 \times 3 \times 2 \text{ mm}^3$ were cut by spark cutting. Before testing the samples were subjected to fine grinding of work surfaces.

Microstructural studies in the case of the TMT workpieces were carried out from the central section of the workpiece parallel to the forging direction. Scanning electron microscopy (SEM) in secondary electron (SE) and

backscattering electron (BSE) modes was used. For the TMT condition, electron backscatter diffraction (EBSD) analysis was performed with a scan-step size of 0.5 μm . EBSD analysis was conducted using the CHANNEL 5 processing software. The grain boundaries having misorientation angle less than 2° were excluded from the consideration taking into account the measurement accuracy. The grain boundaries were assumed as high-angle ones if their misorientation angle was more than 15° . The bright phases of a complex composition precipitated in the superalloy were studied by energy dispersive X-ray (EDX) analysis. In doing so, the ratio of the content of each alloying element in the bright phases to the average content of this element in the superalloy was calculated. Before studying by SEM, the sample surfaces were polished.

3. Results and discussion

3.1. Microstructure characterization

In the initial cast condition, the superalloy had a coarse-grained dendritic structure typical of nickel base superalloys (Fig. 1a). The γ grain size was $d_\gamma \sim 100 \mu\text{m}$. A bright phase was observed along the γ grain boundaries in the form of elongated and equiaxed particles of 0.5–20 μm in size; its volume fraction was about 2.5%. The γ' phase in the cast condition was mainly presented by particles with a size of around 0.25 μm (Fig. 1b). The volume fraction of the γ' phase was about 60% [7].

Fig. 1c, d shows the BSE images of the superalloy after HT. Due to homogenization annealing, the content of alloying elements was equalized in the superalloy volume. As a result, the bright phase was distributed more homogeneously throughout the volume, while its size decreased and the volume fraction increased to 3–4%. The γ grain size was $d_\gamma \sim 100 \mu\text{m}$ as before heat treatment. The γ' precipitates in the form of rounded particles with a size of 0.1–0.25 μm were uniformly distributed in the material; its volume fraction was not changed after HT.

Fig. 1e, f represents the BSE images of the cast superalloy after homogenization and heterogenization annealing. In comparison with the HT condition, the size of the γ grains was not changed, the volume fraction of the bright phase was retained about 3%, the size of the γ' phase increased up to 1–4 μm owing to its coagulation and spheroidization.

The bright phase looked as lamellar and equiaxed precipitates of round or irregular form. EDX analysis of the precipitates revealed that they were strongly enriched, first of all, with tungsten and tantalum and heavily depleted by nickel and aluminum in comparison with the average superalloy composition (Table 1). Thus, the bright phases precipitating in the superalloy have a complex chemical composition enriched with refractory elements (W, Ta, Hf) and depleted by nickel, aluminum and cobalt. A higher content of nickel and cobalt was found in the matrix γ phase, while a higher content of aluminum was detected in the γ' phase. The EDX analysis allows us to conclude that the bright precipitates were topologically close packed (TCP) phases. Note that they often have a negative influence on the mechanical properties of superalloys [9,10].

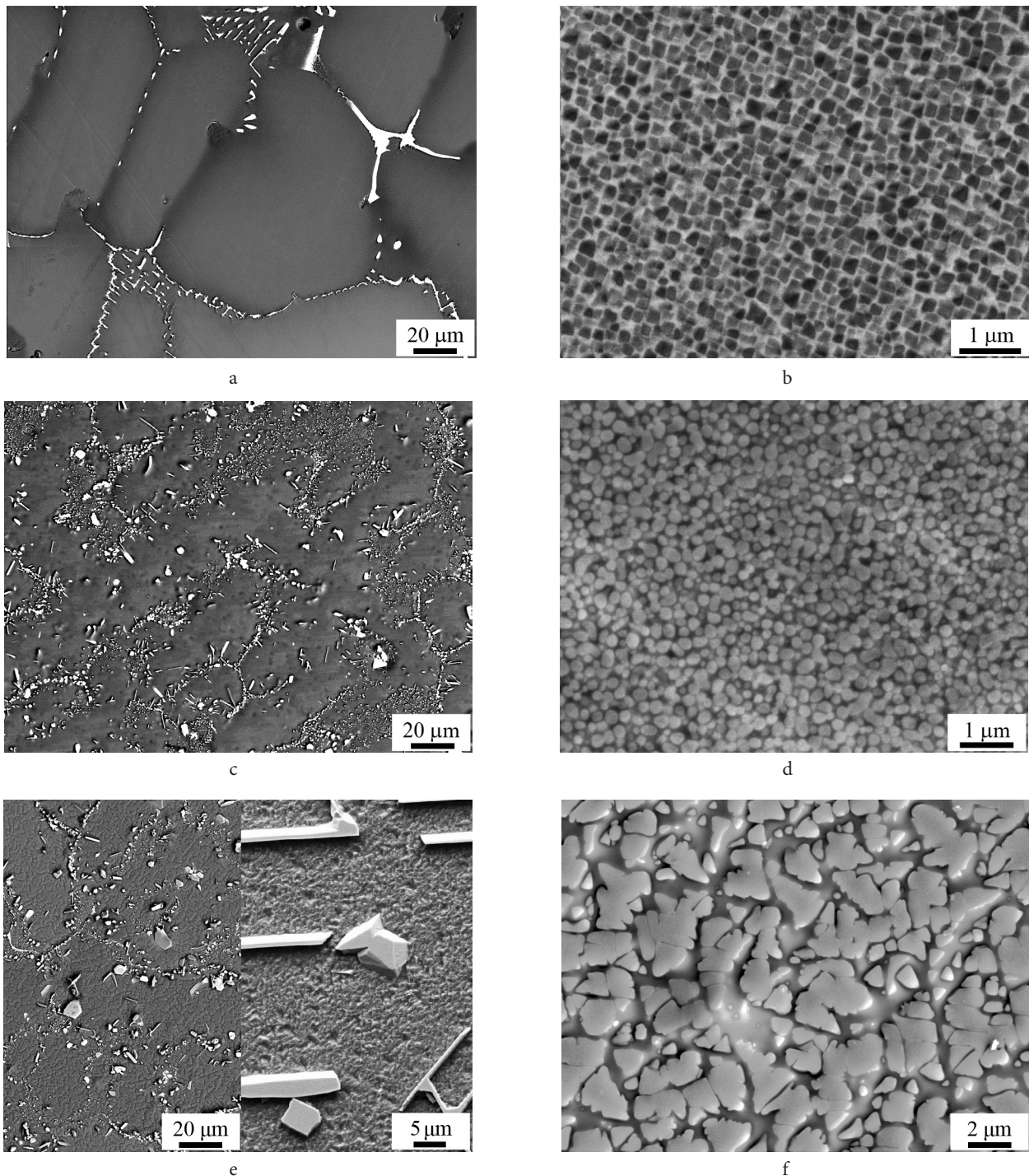


Fig. 1. BSE images obtained for the superalloy SLZhS-1R: in the cast condition (a, b), after homogenization annealing, solid solution heat treatment and ageing (c, d), after homogenization and heterogenization annealing (e, f).

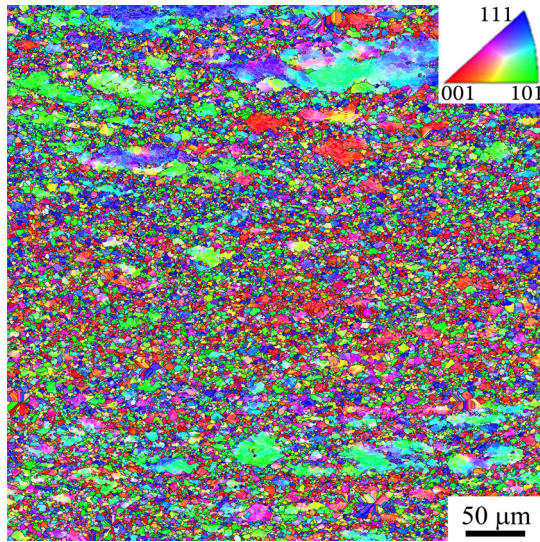
Fig. 2 represents the EBSD orientation map with corresponding misorientation-angle distribution for grain boundaries obtained from the central part of the superalloy workpiece subjected to preliminary homogenization and heterogenization annealing, TMT and ageing. One can see that TMT resulted mainly in a recrystallized microstructure with predominantly high-angle grain boundaries. Non-recrystallized areas up to 100 μm in size were also observed in the microstructure. As was earlier shown on another heavily alloyed nickel base superalloy subjected to similar processing, the main process during forging was continuous dynamic recrystallization [11]. The size of the

recrystallized γ grains was varied in the range of $d = 2 - 50 \mu\text{m}$ (Fig. 2a). It should be noted that the predominantly recrystallized microstructure was obtained almost in the entire volume of the TMT workpiece that was promoted by using the thick-walled can.

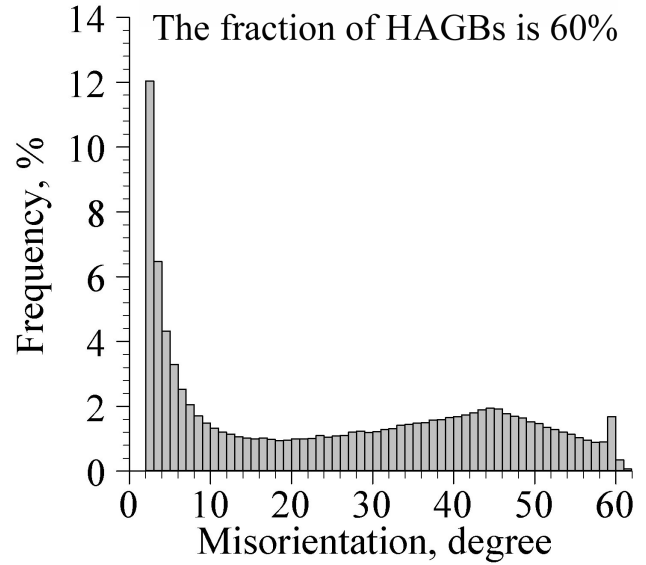
Fig. 3 shows the SE images of the superalloy after TMT and ageing. About 20 vol.% of the γ' phase was presented in the form of large particles of 1–2 μm in size, which were not dissolved during TMT. Fine dispersed γ' phase with a size of 0.1–0.3 μm were precipitated during cooling of the workpiece immediately after forging. The finest dispersed γ' particles with a size of less than 0.1 μm were

Table 1. The ratio of the content of the i -th element (C_i) in the bright phase to the average content of this element (C_i^{av}) in the superalloy defined by EDX analysis.

C_{Ni}/C_{Ni}^{av}	C_{Al}/C_{Al}^{av}	C_{Cr}/C_{Cr}^{av}	C_{Co}/C_{Co}^{av}	C_{Ta}/C_{Ta}^{av}	C_W/C_W^{av}	C_{Hf}/C_{Hf}^{av}	C_C/C_C^{av}
0.17–0.25	0.14–0.17	0.7–1.2	0.45–0.83	3–4	2.5–3.5	1.1–2	1.5–3

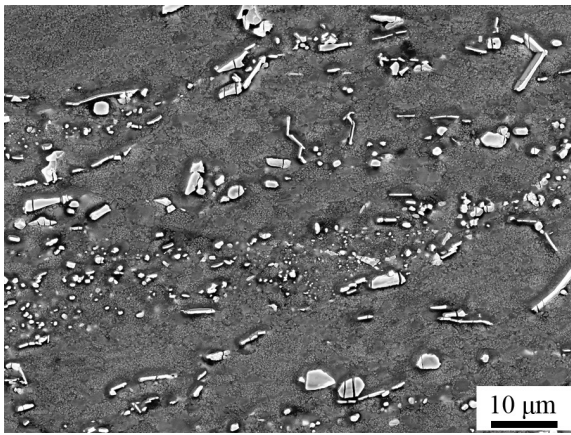


a

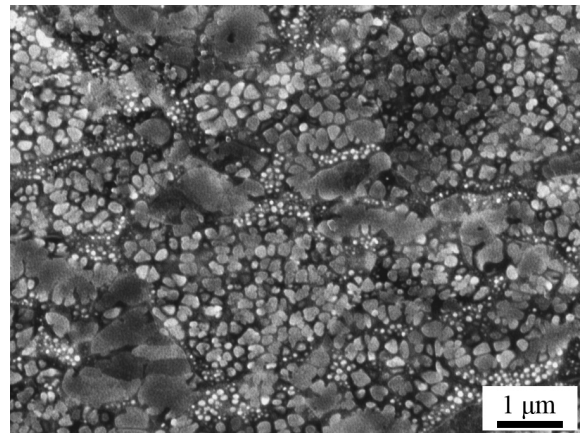


b

Fig. 2. (Color online) EBSD orientation map (a) and corresponding misorientation-angle distribution (b) for grain boundaries obtained from the central part of the superalloy workpiece subjected to thermomechanical treatment ($T=1150^\circ\text{C}$, $\dot{\epsilon}\approx 10^{-2}\text{ s}^{-1}$, $e\approx 1.4$) and ageing (HAGBs — high-angle grain boundaries).



a



b

Fig. 3. SE images obtained from the central part of the superalloy workpiece subjected to thermomechanical treatment ($T=1150^\circ\text{C}$, $\dot{\epsilon}\approx 10^{-2}\text{ s}^{-1}$, $e\approx 1.4$) and ageing.

mainly precipitated in the vicinity of γ grain boundaries as a result of ageing followed by air cooling. Thus, three sizes of the γ' phase were observed in the microstructure. Bright particles of the TCP phases were observed in the TMT condition, their volume fraction was about 5%. Apparently, the TCP phase particles were additionally precipitated during TMT and ageing.

The cast condition subjected to HT and the condition obtained after TMT and ageing were used to prepare the samples for tensile testing.

3.2. Tensile properties

Table 2 represents the tensile properties of the superalloy in the HT and TMT conditions. The tensile properties obtained in the TMT condition were significantly higher than those obtained in the HT condition. The ultimate tensile strength (σ_{UTS}) was 1.4–1.7 times higher, the yield strength was 1.2–1.5 times higher, and the elongation was 2–10 times higher in the TMT condition in contrast to the HT condition.

Table 2. Tensile properties of the SLZhS-1R superalloy in the HT/TMT conditions as compared with those of known superalloys having a similar chemical composition.

Superalloy	T, °C	$\sigma_{0.2}$, MPa	σ_{UTS} , MPa	δ , %
SLZhS-1R (this work)	20	900/1083	1022/1533	4.8/11
	650	810/1069	885/1300	1.1/8.3
	750	665/1027	679/1146	0.5/5.4
VKLS-20 [4]	20	740	1500	-
Cotac-744 [12]	20	-	1505	13
Cotac-74 [12]	20	-	1505	12.4

Thus, despite the presence of a rather significant volume fraction of TCP phases, the tensile properties of the SLZhS-1R superalloy can be significantly improved by TMT. This should be attributed to the relatively fine-grained structure obtained by TMT, the high content of the γ' phase, and the solid-solution hardening due to the heavy alloying with substitution elements (W, Co, Cr). Probably, the TCP phases also contributed to the hardening. The refined microstructure obtained after TMT provided not only improved tensile properties in comparison with the cast and HT condition but also quite competitive properties in comparison with those of known heat-resistant nickel base superalloys having a similar chemical composition (Table 2).

4. Conclusions

In the present work, the novel heavily alloyed nickel base superalloy SLZhS-1R (Ni-47(Al, Cr, Co, Ta, W, Hf)-0.2(C, B) (wt.)) developed at PJSC “UEC-Saturn” using computer design and intended for application at operating temperatures up to 800°C has been investigated. The as-cast ingots were subjected to HT or TMT and ageing. The following conclusions can be drawn:

- after preliminary homogenization and heterogenization annealing the cast superalloy workpieces were successfully forged under quasi-isothermal conditions at temperatures below the γ' solvus temperature using a special thick-walled can. This ensured the uniform development of recrystallization processes in the workpieces that led to formation of a relatively fine-grained recrystallized structure;
- in the TMT condition the superalloy had a smaller size of γ grains but a larger average size of the γ' precipitates than in the HT condition. In the both superalloy conditions there were TCP phases in the amount of up to 5 vol.%;
- in the TMT condition the superalloy showed significantly higher tensile properties than in the HT condition. The ultimate tensile strength of the superalloy in the TMT condition was 40–70% higher than that in the HT condition, while the ductility in the TMT condition was also significantly higher. The tensile properties of the SLZhS-1R superalloy in the TMT condition were comparable with the properties of the known heat-resistant nickel base superalloys having a similar composition.

Acknowledgements. The present work was supported by the Russian Science Foundation (Grant No. №18-19-00594). The work was performed using the facilities of the shared

services center “Structural and Physical-Mechanical Studies of Materials” at the Institute for Metals Superplasticity Problems of Russian Academy of Sciences.

References

1. R.C. Reed. The superalloys: Fundamentals and Applications. Cambridge University Press (2006) 372 p. [Crossref](#)
2. M.C. Kushan, S.C. Uzgur, Y. Uzunonut, F. Diltemiz. Recent Advances in Aircraft Technology. Croatia, InTech Rijeka (2012) pp. 75–96.
3. O.A. Kaibyshev, F.Z. Utyashev. Sverkhplastichnost', izmel'cheniye mikrostruktury i obrabotka trudnodeformiruyemykh splavov. Moscow, Nauka (2002) 438 p. (in Russian)
4. A.V. Logunov. Zharoprochnyye nikelovyye splavy dlya lopatok i diskov gazovyykh turbin. Rybinsk, LLC Publishing House “Gazoturbinnyye tekhnologii” (2017) 854 p. (in Russian)
5. R.A. Hobbs, S. Tin, C.M.F. Rae. Metall. Mater. Trans. A. 36, 2761 (2005). [Crossref](#)
6. S. Tin, L. Zhang, R.A. Hobbs, A.-C. Yeh, C.M. F. Rae, B. Broomfield. In: Superalloys 2008 (Ed. by R. C. Reed, P. Caron, T. Gabb, E. Huron, S. Woodare). TMS, Warrendale, Seven Springs, PA, USA (2008) pp. 81–90.
7. R.V. Shakhov, A.A. Ganeev, Sh.Kh. Mukhtarov, A.V. Logunov, V.M. Imayev, R.M. Imayev. IOP Conference Series: Mater. Sci. & Eng. 447 (2018) 012045. [Crossref](#)
8. R.V. Shakhov, A.A. Ganeev, Sh.Kh. Mukhtarov, A.V. Logunov. Letters on Materials. 8 (4), 494 (2018). [Crossref](#)
9. R.M. Nazarkin, V.G. Kolodochkina, O.G. Ospennikova, M.R. Orlov. Electronic scientific journal “Proceedings of VIAM”. 12, 22 (2015). (in Russian)
10. T. Sugui, W. Minggang, L. Tang, Q. Benjiang, X. Jun. Mater. Sci. Eng. A. 527, 5444 (2010). [Crossref](#)
11. Sh.Kh. Mukhtarov, V.M. Imayev, A.V. Logunov, Yu.N. Shmotin, A.M. Mikhailov, R.A. Gaisin, R.V. Shakhov, A.A. Ganeev, R.M. Imayev. Mater. Sci. & Technol. 35 (13), 1605 (2019). [Crossref](#)
12. T. Khan, J.F. Stohr, H. Bibring. In: Superalloys 1980 (Ed. by J.K. Tien, S.T. Wlodek, H. III Morrow, M. Gell, G.E. Maurer). ASM, Champion, PA, USA (1980) pp. 531–540. [Crossref](#)